ELSEVIER

Journal of Nuclear Materials 247 (1997) 161–171

journal of nuclear materials

Section 5. Back end and fuel cycle

Transpiration studies on the volatilities of $PuO_3(g)$ and $PuO_2(OH)_2(g)$ from $PuO_2(s)$ in the presence of steam and oxygen and application to plutonium volatility in mixed-waste thermal oxidation processors

Oscar H. Krikorian, Alfred S. Fontes Jr., Bartley B. Ebbinghaus, Martyn G. Adamson *

University of California, Lawrence Livermore National Laboratory, Livermore, CA 94551, USA

Abstract

Transpiration experiments have been carried out to study the volatility of $PuO_2(s)$ in the presence of oxygen and steam. Vapor pressures have been measured for $PuO_3(g)$ and $PuO_2(OH)_2(g)$ and thermodynamic data established for them. Thus, $\Delta_f H^0_{298}$ is determined to be $-(562.8 \pm 5.0)$ kJ/mol for $PuO_3(g)$ and $-(1{,}018.2 \pm 3.3)$ kJ/mol for $PuO_2(OH)_2(g)$. In applying the Pu volatility data to a pilot scale mixed waste (containing both radioactive and hazardous constituents) incinerator with primary and secondary combustion chambers, it is found that Pu volatilization makes a negligible contribution to air emissions if the temperature in the secondary combustor is maintained at less than 1600 K. Chlorine- and fluorine-induced volatilities of plutonium are not considered in this analysis. © 1997 Elsevier Science B.V.

1. Introduction

The overall objective in this work was to conduct experimental studies to identify the types and amounts of volatile gaseous species of Pu that are produced in the offgases of mixed-waste thermal oxidation processors. This data would then be used in engineering models to estimate or bound Pu emissions to the atmosphere from a particular thermal oxidation process. Although the data are useful for any thermal process using actinides, the study was conducted primarily to address safety concerns in treating mixed waste by incineration and other alternative thermal treatment processes. In this study, the extent of Pu volatility produced from $PuO_2(s)$ in the presence of steam and oxygen was established. Pu volatilization induced by chlorine and by fluorine is expected to be important and needs to be addressed in future work.

Studies on toxic metal emissions from incinerators show that the metals that vaporize in the incinerator combustion chamber preferentially condense onto very fine fly ash particulates or form aerosols that are carried by the offgas [1,2]. These particulates are in a size range (< 1 μm) that are difficult to remove with air pollution control devices. Complete removal is not possible in flow systems, even with HEPA filters. A knowledge of the volatility levels of Pu produced in the thermal oxidizer offgas is needed for proper design to eliminate the possibility of Pu emissions at unacceptable levels.

Earlier experiments using the transpiration method were conducted to determine Pu volatilities from $^{239}PuO_2(s)$ in the presence of steam and oxygen [3]. The volatility of Pu species was found to be very low, e.g., $< 10^{-10}$ bar at 1300 K. These data only provided an approximate upper limit to Pu volatility. The results indicated that $PuO_2(s)$ dust transport occurred in most of the runs, and a significant amount of Pu contamination from the glovebox environment occurred during handling of silica wool collectors used to sample the volatilized Pu. New studies were initiated to obtain more quantitative results [4]. This included using $^{238}PuO_2(s)$ to obtain better sensitivity of detection by alpha-counting, and a collector tube instead of silica wool for sample collection in order to avoid sample contamination from the glovebox environment. A few runs were also made with $^{239}PuO_2(s)$. Measurements have now been completed and the overall data summarized in this report.

* Corresponding author. Tel.: +1-510 423 2024; fax: +1-510 423 8700; e-mail: adamson1@llnl.gov.

PII S0022-3115(97)00043-3

2. Experimental

2.1. Transpiration method

In the transpiration method, [5] a known amount of carrier gas is slowly passed over a solid or liquid in a furnace chamber, such that any volatile gases produced become entrained in the carrier gas and are swept out of the chamber where the volatilized gas is then condensed and analyzed. The carrier gas may also contain reactive gases that contribute to forming the volatilizing species, such as, for the reaction,

$$PuO_2(s) + 1/2O_2(g) + H_2O(g) = PuO_2(OH)_2(g), \quad (1)$$

where $O_2(g)$ and $H_2O(g)$ are both reactive gases that contribute to production of $PuO_2(OH)_2(g)$. Variation of flow rate of the carrier gas permits one to establish the conditions under which the carrier gas becomes saturated with the equilibrium vapor pressure of the volatilizing species. At too slow a flow rate, diffusional transport of the volatilized gas out of the furnace chamber results in values apparently higher than the equilibrium vapor pressure. At too high a flow rate, the residence time of the carrier gas in the furnace chamber is not long enough for saturation with the equilibrium vapor pressure to occur, and results in pressure values that are too low. At intermediate flow rates, a 'plateau' region is established where the equilibrium vapor pressure persists over a range of flow rates. The vapor pressure of the volatilized gas under equilibrium conditions is determined from the ideal gas law by taking the ratio of moles of volatilized species to total moles of gas passed through the chamber to be proportional to the partial pressure of volatilized species to total pressure of the carrier gas passed. The transpiration method may also be used to obtain information on the formula of the volatilizing species. This is done by varying the partial pressures of the reactive gases and noting the law of mass action effects on the volatilizing species. Thus, for the reaction above, the equilibrium partial pressure of $PuO_2(OH)_2(g)$ is expected to be proportional to the $1/2$ power of the $O_2(g)$ pressure and to the first power of the $H_2O(g)$ pressure. If the volatilizing species were different than $PuO_2(OH)_2(g)$, then the power dependence on $O_2(g)$ and $H_2O(g)$ would be accordingly different depending upon the equation stoichiometry.

2.2. Experimental description

The transpiration apparatus is illustrated schematically in Fig. 1. It used a Thermcraft Kanthal-heater clamshell furnace rated to 1200°C in air, that provided a uniform-temperature hot zone ≈ 7 cm long and an overall heated zone ≈ 20 cm long. The furnace tube was of silica glass, 2.6 cm OD × 38.5 cm long with end caps mounted on 35/25 silica glass ball and socket end joints sealed with silicone grease. An 8 mm OD silica glass gas inlet tube was mounted as a sidearm just inside of the end cap seal on the upstream side. A thermocouple probe tube made of 7 mm OD silica glass tubing closed at the end was mounted on the upstream endcap and extended to the center of the hot zone. A silica glass wool insulating plug, 1.5 cm long, was mounted around the thermocouple probe tube up to the beginning of the uniform temperature hot zone. A 9 mm OD × 12 cm long gas outlet and collector tube extended from the downstream side of the uniform temperature hot zone to a 12/30 standard taper joint. The tubing then continued through the end cap. A silica wool insulating plug, 1.5 cm long, was mounted around the inlet end of the collector tube. The standard taper joint was sealed with MoS_2 lubricant, which provided for ease of disassembly when removing the collector tube after a heating. A fused silica boat, 2.0 cm wide × 4.0 cm long × 0.9 cm high was used for the $^{238}PuO_2(s)$ sample, and an Al_2O_3 combustion boat (from Atomergic), 1.7 cm wide ×

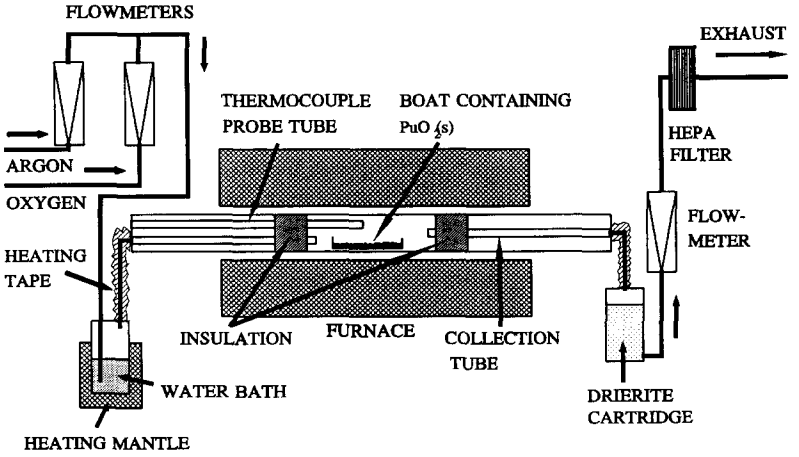

Fig. 1. Schematic of the apparatus used for the transpiration studies of volatilization of $PuO_2(s)$ in the presence of oxygen and steam.

5.0 cm long × 0.7 cm high, was used for the $^{239}PuO_2$(s) sample. Temperatures were measured with type-K thermocouples with inconel sheaths. One thermocouple was located on the outside of the furnace tube at its center, and two thermocouples were located in the silica glass thermocouple probe tube just above the sample boat. These various thermocouples were periodically checked and calibrated against two type-S reference thermocouples. A water saturator was located upstream of the furnace. The water saturator was made of a 6 mm thick wall Al vessel with an 800 cm^3 capacity and provided with a fritted stainless steel disperser for the carrier gas, which disperser was located 1 cm above the bottom of the vessel. Water level was maintained at 500–600 cm^3 during the runs. The vessel was heated with a Glas–col mantle. A desiccant cartridge loaded with Drierite ($CaSO_4$) was located downstream of the furnace. The cartridge was provided with disconnect fittings to allow weighing to determine water pickup accumulated during a run. Gas lines from the water saturator to the furnace and from the furnace to the Drierite cartridge were of stainless steel. Valves were also of stainless steel with Viton rubber seals. Either Viton o-ring compression fittings, or stainless steel to silica glass ball joints were used to connect with the furnace tubes. Heating tapes were wrapped on the lines from the water saturator to the furnace tube, and from the furnace tube to the Drierite cartridge and maintained at ~ 150°C during the runs to prevent water condensation. Precision Flow Devices PFD-401 mass flow controllers were used to control O_2 and Ar flow inputs and to monitor the output gas flow. Flow rates were measured in cm^3/min STP. Calibrations for these flow controllers were provided by the supplier. The flow controllers were compared periodically with others to check for any changes in calibrations. Weighing were carried out on an Ohaus GT 2100 electronic balance with a capacity of 2100 g and an accuracy of ±0.01 g. Certified weights were used periodically to check the balance calibrations.

The $^{238}PuO_2$(s) was obtained as sintered chunks. It was a reactor produced material with an isotopic content of 77.60% ^{238}Pu, 16.05% ^{239}Pu, 2.48% ^{240}Pu, 0.39% ^{241}Pu, 0.18% ^{242}Pu, and 3.3% ^{234}U, all on the basis of at.% of metal content. Prior to use, the $^{238}PuO_2$(s) was ground to a powder with a mortar and pestle. In runs prior to the first run reported here, run # 77, the sample was heated for 52 h in steam and oxygen at temperatures of 824 to 1277 K. The $^{239}PuO_2$(s) was obtained as a fine powder that had been formed from electrorefined Pu. It had an isotopic content of 0.014% ^{238}Pu, 93.819% ^{239}Pu, 5.870% ^{240}Pu, 0.211% ^{241}Pu, 0.049% ^{242}Pu, and 0.037% ^{241}Am, all on the basis of at.% of metal content. Prior to making the runs, the sample was heated for 4 hours in oxygen at 1432 K. Earlier work, runs 1 to 78, are reported elsewhere [3,4]. They included experiments on plutonium. Runs 81 to 84, 89, 90, and 97 were incomplete, contaminated, or unrelevant to this study and are not reported here.

Analyses of the deposits in the silica glass collector tubes were carried out as follows. The deposits were dissolved by slowly flowing warm concentrated HF through the insides of the tubes to leach out the inner surfaces of the tubes. This was followed by 6 N HCl and water rinses. By dissolving out only the insides of the tubes, we avoided Pu contamination from the outsides of the tubes that could occur during handling. An aliquot of the solution was dried on a platinum planchet and counted for total alpha dpm using a gas proportional counter with an efficiency of 52%. Appropriate corrections were made for counter background. Pulse height analysis was also used on these samples to evaluate the presence of impurity alpha emitters. Thus, the amount of ^{234}U as well as ^{238}Pu was determined in the $^{238}PuO_2$(s) runs. Corrections were made for isotopic alpha contributions to obtain total Pu. The data are generally accurate to within ±5%.

The experimental procedure used was as follows. A new furnace tube was used for each series of runs. The boat containing PuO_2(s) was placed in position in the furnace tube, displaced 1.5 cm to the upstream side of the centerline of the hot zone. A silica wool plug, if used, was then placed in position immediately downstream of the boat. The boat and plug would then be left in position until the end of the series of runs. A new collector tube was mounted in position and the system sealed up for the run. The water bath was brought up to constant temperature with the valve open to the air and the heating tapes were brought up to temperature. An initial weighing was taken of the Drierite cartridge. Gas flow (without water) through the furnace was started while bypassing the water bath and Drierite cartridge. The furnace was brought up to temperature, requiring ≈ 30 min to go from room temperature to the temperature of the run. When the run temperature was reached, the water bath was valved off from the air, and gas was flowed through the water bath, then through the furnace and through the Drierite cartridge (when H_2O was used), and through the exit flow meter. Upon completion of the run, the gas flow was diverted to bypass the water bath and Drierite. The furnace was turned off and the gas flow then stopped, allowing the furnace chamber to cool in stagnant gas open through long piping to the glovebox air. The Drierite was again weighed to obtain the amount of water pickup. After cooldown, the collector tube was carefully removed into a clean plastic bag and sent in for analysis.

3. Analysis of results

The transpiration data for Pu volatility are summarized in Table 1. The total pressure of Pu species is included in the table by calculation from the amount of Pu collected, assuming a single atom of Pu to be present in each volatile species. The steam pressures for most of the runs are based upon the amount of water collected in the Drierite. For a

few runs where weighing problems were encountered, the steam pressures are based upon the water bath temperatures. Agreement between the amount of steam expected from the water bath temperature and the amount collected on the Drierite for all the runs was generally within ±5%. Flow rates of gas ranged from 11.6 to 147.0 cm^3/min STP for the various runs, with flow rates typically at ≈ 50 cm^3/min STP. These flow rates were expected to be within the plateau region based on similar experiments on reactions of U_3O_8(s) with steam and oxygen [4]. Therefore, the Pu volatility data were taken to represent equilibrium values.

The possibility of PuO_2(s) dust transport is important to consider in these experiments. In earlier studies on PuO_2/ash samples [4], the samples were ground in a mortar and pestle before every run. A silica wool dust filter was used on those runs and experimental conditions were similar to the current runs. Several nanograms of Pu transport occurred in each of those runs, which can be attributed to dust transport. On the first run with $^{238}PuO_2$(s) in this earlier study [4], which was run at 824 K after grinding the sample, 4 ng of Pu was transported. No further grinding was used for later runs. On the second run on $^{238}PuO_2$(s) at 1076 K, 0.008 ng of Pu was transported. For the next 22 runs at temperatures up to 1325 K, the amount of Pu transport was typically on the order of 0.01 ng. For runs that followed at higher temperatures, the Pu transport levels were higher, as would be expected from Pu volatilization. However, for a run under argon flow only, at 1485 K, the Pu transport was only 0.01 ng, which indicates little if any dust transport or Pu volatility occurred. For the $^{239}PuO_2$(s) powder sample used in this

Table 1
Transpiration data for Pu volatility from $^{238}PuO_2$(s) and $^{239}PuO_2$(s)

Run #	T (K)	Time (min)	Tot. mol gas	$p(O_2)$ (bar)	$p(H_2O)$ (bar)	p(Ar) (bar)	Pu (ng)	p(Pu total) (bar)
$^{238}PuO_2$(s):								
77	1327	600	2.645	0.475	0.538		0.0348	5.59×10^{-14}
78	1325	600	1.239	1.013			0.0313	1.07×10^{-13}
79	1327	840	1.732	0.508		0.506	0.0006	1.54×10^{-15}
80	1326	1050	2.169	0.253		0.760	0.0035	6.92×10^{-15}
85	1326	480	2.126	0.472	0.541		0.0159	3.18×10^{-14}
86	1326	600	1.239	1.013			0.0022	7.52×10^{-15}
87	1326	890	1.835	0.508		0.506	0.0007	1.67×10^{-15}
88	1326	860	1.776	0.253		0.760	0.173	4.13×10^{-13}
91	1326	600	3.934	0.064	0.719	0.230	0.72	7.79×10^{-13}
92	1326	600	1.751	0.144	0.354	0.510	0.115	2.80×10^{-13}
93	1325	600	1.402	0.179	0.188	0.645	0.0018	5.47×10^{-15}
94	1326	300	0.626	0.201	0.090	0.722	0.00624	4.25×10^{-14}
95	1325	600	3.855	0.065	0.713	0.235	0.0121	1.34×10^{-14}
96	1325	570	1.194	0.200	0.094	0.719	0.0088	3.14×10^{-14}
105 [a]	1482	120	0.517	0.485	0.528		19.2	1.58×10^{-10}
106 [a]	1482	120	0.248	1.013			2.48	4.26×10^{-11}
107 [a]	1483	240	0.124	1.013			1.59	5.46×10^{-11}
108 [a]	1482	120	0.758	0.066	0.708	0.239	21.5	1.21×10^{-10}
109 [a]	1483	120	0.345	0.146	0.342	0.525	8.03	9.92×10^{-11}
110 [a]	1483	120	0.277	0.181	0.179	0.653	4.21	6.46×10^{-11}
111 [a]	1483	360	0.186	1.013			1.11	2.54×10^{-11}
112	1486	120	0.499	0.503	0.511		5.66	4.82×10^{-11}
113	1487	120	0.248	1.013			0.0429	7.37×10^{-13}
114	1485	240	0.124	1.013			0.0353	1.22×10^{-12}
115	1486	120	0.496	0.253	0.760		0.121	1.03×10^{-12}
116	1485	110	0.228			1.013	0.0127	2.37×10^{-13}
$^{239}PuO_2$(s):								
98	1431	240	0.496	1.013			0.327	2.80×10^{-12}
99	1431	240	0.495	0.508		0.506	< 0.025	$< 2.14 \times 10^{-13}$
100	1431	480	0.992	0.253		0.760	< 0.19	$< 8.13 \times 10^{-13}$
101	1431	240	1.507	0.067	0.706	0.240	0.40	1.12×10^{-12}
102	1431	240	0.712	0.141	0.365	0.508	1.2	7.14×10^{-12}
103	1431	480	1.103	0.182	0.175	0.656	0.628	2.41×10^{-12}
104 [a]	1431	240	1.060	0.474	0.539		30	1.20×10^{-10}

[a] These runs were made without a silica glass wool dust filter.

present study, an initial heating was carried out at 1432 K for 4 h without a Pu transport determination. Subsequent runs (without grinding) show very low Pu transport consistent with data from the $^{238}PuO_2$(s) runs. These observations indicate that dust transport through the silica wool filter is a problem in the initial heating if the sample used contains fine particulates, such as results from grinding in a mortar and pestle. However, subsequent heating no longer shows evidence of dust transport through the silica wool filter. It is believed that sufficient sintering had occurred in the PuO_2(s) samples used in these subsequent experiments that dust transport was not a problem with or without the use of a silica wool filter.

To analyze the data for identification of species, it is expected, in analogy to uranium volatility behavior [4,9], that volatilization can occur to both PuO_3(g) and $PuO_2(OH)_2$(g) species when steam and oxygen are present. Any volatilization to the known plutonium oxide species, PuO(g) and PuO_2(g), will be insignificant relative to the amounts of volatility observed in these experiments, according to the known thermodynamic data [6].

The volatilization reactions and the associated equilibrium constants are

$$PuO_2(s) + 1/2O_2(g) = PuO_3(g), \quad (2)$$

$K_1 = p(PuO_3)/a(PuO_2)p(O_2)^{1/2}$,

$PuO_2(s) + 1/2O_2(g) + H_2O(g) = PuO_2(OH)_2(g)$, Eq. (1),

$K_2 = p(PuO_2(OH)_2)/a(PuO_2)p(O_2)^{1/2}p(H_2O)$.

Taking the activity of PuO_2(s) as unity, and combining the equilibrium constant expressions, the following relationship is obtained:

$$\left[p(PuO_3) + p(PuO_2(OH)_2)\right]/p(O_2)^{1/2}$$

$$= p(\text{Pu total})/p(O_2)^{1/2} = K_1 + K_2 p(H_2O). \quad (3)$$

This expression shows that if $PuO_2(OH)_2$(g) is present in addition to PuO_3(g), p(Pu total)/$p(O_2)^{1/2}$ will have a linear dependence on steam pressure. Data are shown for a series of runs made without the silica wool dust filter, at 1483 K with oxygen pressures of 0.06 to 1 bar and steam pressures of 0 to 0.7 bar (see Fig. 2). The data, although limited, confirm the presence of $PuO_2(OH)_2$(g). A sufficient number of accurate measurements were not made with variable oxygen pressures (with steam absent) to establish the PuO_3(g) species. However, PuO_3(g) is the only other likely species in addition to $PuO_2(OH)_2$(g) in these experiments. PuO(g) and PuO_2(g) vapor pressures are known to be much lower under these conditions [6] and the reproducibility of the data suggest that it is not dust contamination.

In examining the volatility data, it is found that the runs made without the silica wool dust filter show significantly higher volatilities than those with the filter in place. This is interpreted to mean that the Pu vapor species interacted with the silica wool. Possible interactions would include

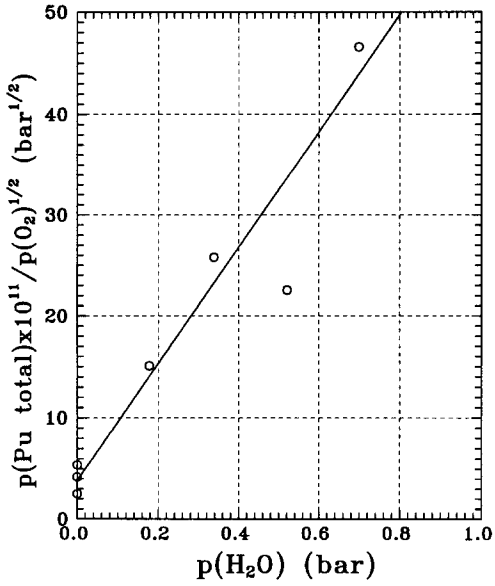

Fig. 2. Plot of p(Pu total)/$p(O_2)^{1/2}$ versus $p(H_2O)$ at 1483 K. The plot increases linearly, which indicates that $PuO_2(OH)_2$ is formed in the vapor.

the dissolution of PuO_2 in solid solution in SiO_2(gl) or the formation of a plutonium silicate compound. For convenience, this unknown product is referred to as $PuO_2 \cdot xSiO_2$(s) where x is extremely large and not necessarily the same between experiments and not necessarily the same throughout a particular experiment. The volatilization reactions for the experiments with the silica wool filters in place are then

$$PuO_2 \cdot xSiO_2(s) + 1/2O_2(g) = xSiO_2(gl) + PuO_3(g), \quad (4)$$

and

$$PuO_2 \cdot xSiO_2(s) + 1/2O_2(g) + H_2O(g)$$

$$= xSiO_2(gl) + PuO_2(OH)_2(g). \quad (5)$$

Since the silica wool filter is fully within the constant temperature hot zone of the furnace, the PuO_3(g) and $PuO_2(OH)_2$(g) exiting the silica wool can be treated as equilibrium vapor pressures thus allowing the calculation of the average reduction in volatility due to the presence of the silica wool. Within the main furnace chamber, the supply of PuO_2(s) is apparently sufficient to replenish Pu gaseous species lost to the silica walls, so that a close approach to equilibrium can be attained for the Pu gaseous species with PuO_2(s) for the runs made without the silica wool filter.

Values of $(\Delta G_T^0 - \Delta H_{298}^0)/T$ versus temperature are summarized in Table 2 for Eqs. (1), (2), (4) and (5). The $(\Delta G_T^0 - \Delta H_{298}^0)/T$ values for Eqs. (1) and (2) are obtained from $(G_T^0 - H_{298}^0)/T$ values for PuO_2(s), O_2(g),

Table 2
Free energy functions for the reactions Eqs. (1), (2), (4) and (5) $-(\Delta G_T^0 - \Delta H_{298}^0)/T$, J/mol K

T (K)	Reac. Eq. (2) or Eq. (4)	Reac. Eq. (1) or Eq. (5)
800	141.739	16.534
900	140.390	15.762
1000	139.063	15.000
1100	137.763	14.246
1200	136.488	13.497
1300	135.242	12.756
1400	134.022	12.020
1500	132.829	11.289
1600	131.663	10.566
1700	130.524	9.849
1800	129.408	9.135
1900	128.317	8.431
2000	127.249	7.730

and $H_2O(g)$ from Cordfunke et al. [6], and for $PuO_3(g)$ and $PuO_2(OH)_2(g)$ from Ebbinghaus [7]. Eq. (4) is estimated to have the same ΔS_{298}^0 and ΔC_p as Eq. (2), and hence has the same $(\Delta G_T^0 - \Delta H_{298}^0)/T$ values. Similarly, Eq. (5) has the same $(\Delta G_T^0 - \Delta H_{298}^0)/T$ values as Eq. (1).

The data with only oxygen gas present are used to obtain $PuO_3(g)$ volatilities from $PuO_2(s)$. The analysis is summarized in Table 3 for Eq. (1), i.e., in runs without the silica wool filter. Data for $p(PuO_3)$ and $p(O_2)$ are taken from Table 1 and $(\Delta_r G_T^0 - \Delta_r H_{298}^0)/T$ values from Table 2. An average $\Delta H_{r,298}^0$ of (493.0 ± 4.9) kJ/mol is obtained for the reaction, where the uncertainty is the least squares uncertainty. Taking $\Delta_f H_{298}^0 = -(1{,}055.8 \pm 1.0)$ kJ/mol for $PuO_2(s)$ [6], $\Delta_f H_{298}^0 = -(562.8 \pm 5.0)$ kJ/mol is obtained for $PuO_3(g)$. Data for Eq. (2) is illustrated in Fig. 3 in terms of a log K_{eq} versus $1/T$ plot.

For volatilization of $PuO_3(g)$ from $PuO_2 \cdot xSiO_2(s)$ in runs with oxygen gas using the silica wool filter, i.e., Eq. (4), the analysis is summarized in Table 4. $\Delta_r H_{298}^0$ for the reaction is found to be (528.2 ± 22.5) kJ/mol. Data for Eq. (4) are illustrated in Fig. 3 in terms of a log K_{eq} versus $1/T$ plot. The Eq. (4) data points show a substantial amount of scatter, but show about a factor of 20 reduction in $PuO_3(g)$ pressures compared with Eq. (2).

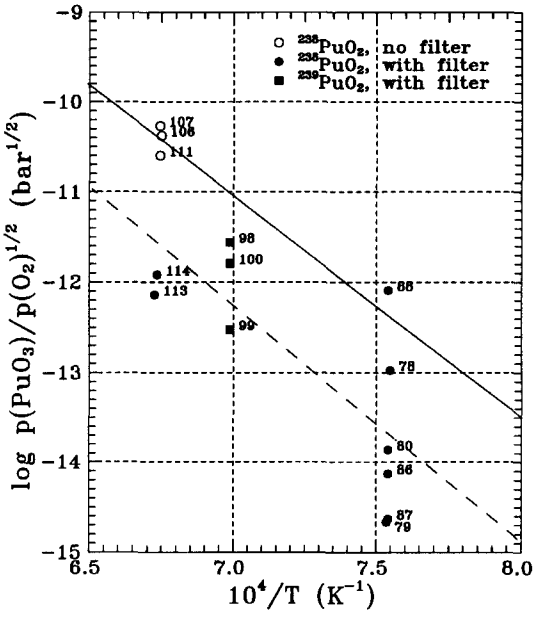

Fig. 3. Plots of log $p(PuO_3)/p(O_2)^{1/2}$ versus $1/T$ for the reactions: $PuO_2(s) + 1/2O_2(g) = PuO_3(g)$ (with no silica glass wool filter) and $PuO_2 \cdot xSiO_2(s) + 1/2O_2(g) = xSiO_2(gl) + PuO_3(g)$ (with silica glass wool filter).

The data are now analyzed for $PuO_2(OH)_2(g)$ volatility from $PuO_2(s)$, i.e., Eq. (1), with both oxygen and steam present and without the silica wool filter (see Table 5). Here, the thermodynamic data from Eq. (2) are used to calculate $p(PuO_3)$ for each data point. Next $p(PuO_3)$ is subtracted from p(Pu total) to obtain $p(PuO_2(OH)_2)$. K_{eq} is then determined using appropriate values of $p(O_2)$ and $p(H_2O)$. $PuO_2(OH)_2(g)$ pressures are found to be substantially higher than the $PuO_3(g)$ pressures under these conditions, hence giving more accurate values for $p(PuO_2(OH)_2)$ than for $p(PuO_3)$. The data are illustrated in Fig. 4 as a log K_{eq} versus $1/T$ plot. $\Delta_r H_r^0$ for Eq. (1) was found to be (279.5 ± 3.1) kJ/mol. Taking $\Delta_f H_{298}^0 = -(1{,}055.8 \pm 1.0)$ kJ/mol for $PuO_2(s)$ [6] and $\Delta_f H_{298}^0 = -(241.83 \pm 0.04)$ kJ/mol for $H_2O(g)$ [6], gives $-(1{,}018.2 \pm 3.3)$ kJ/mol for $\Delta_f H_{298}^0$ of $PuO_2(OH)_2(g)$.

Table 3
Analysis of thermodynamic data for the reaction $PuO_2(s) + 1/2O_2(g) = PuO_3(g)$

Run #	T (K)	K_{eq} (J/mol K)	$\Delta_r G_T^0/T$ (J/mol K)	$(\Delta_r G_T^0 - \Delta_r H_{298}^0)/T$ (kJ/mol)	$\Delta_r H_{298}^0$
$^{238}PuO_2(s)$, without filter:					
106	1482	4.23×10^{-11}	198.61	−133.20	491.74
107	1483	5.43×10^{-11}	196.54	−133.19	488.99
111	1483	2.53×10^{-11}	202.90	−133.19	498.42
				ave.	493.0 ± 4.8

Table 4
Analysis of thermodynamic data for the reaction $PuO_2 \cdot xSiO_2(s) + 1/2\ O_2(g) = xSiO_2(gl) + PuO_3(g)$

Run #	T (K)	K_{eq} (J/mol K)	$\Delta_r G_T^0/T$ (J/mol K)	$(\Delta_r G_T^0 - \Delta_r H_{298}^0)/T$ (kJ/mol)	$\Delta_r H_{298}^0$
$^{238}PuO_2$(s), with filter:					
78	1325	1.07×10^{-13}	248.35	−135.10	508.07
79	1327	2.15×10^{-15}	280.79	−135.07	551.85
80	1326	1.38×10^{-14}	265.39	−135.08	531.02
86	1326	7.47×10^{-15}	270.46	−135.08	537.75
87	1326	2.35×10^{-15}	280.09	−135.08	550.52
88	1326	8.21×10^{-13}	231.38	−135.08	485.93
113	1487	7.32×10^{-13}	232.34	−133.14	543.47
114	1485	1.21×10^{-12}	228.20	−133.17	536.62
$^{239}PuO_2$(s), with filter:					
98	1431	2.78×10^{-12}	221.25	−133.81	508.09
99	1431	$< 3.01 \times 10^{-13}$	> 239.71	−133.81	> 534.54 [a]
100	1431	$< 1.61 \times 10^{-12}$	> 225.76	−133.81	> 514.55 [a]
				ave.	528.2 ± 22.5

[a] These values are not included in determining the average $\Delta_r H_{298}^0$.

Table 5
Analysis of thermodynamic data for the reaction $PuO_2(s) + 1/2O_2(g) + H_2O(g) = PuO_2(OH)_2(g)$

Run #	T (K)	p(Pu total) (bar)	Calc. $p(PuO_3)$ (bar)	Diff. $p(PuO_2(OH)_2)$ (bar)	K_{eq} (J/mol K)	$\Delta G_{r,T}^0/T$ (kJ/mol)	$\Delta H_{r,298}^0$
$^{239}PuO_2$(s), without filter:							
104	1431	1.20×10^{-10}	6.77×10^{-12}	1.13×10^{-10}	3.05×10^{-10}	182.18	277.66
$^{238}PuO_2$(s), without filter:							
105	1482	1.58×10^{-10}	2.65×10^{-11}	1.32×10^{-10}	3.58×10^{-10}	180.84	285.02
108	1482	1.21×10^{-10}	9.80×10^{-12}	1.10×10^{-10}	6.08×10^{-10}	176.43	278.49
109	1483	9.92×10^{-11}	1.49×10^{-11}	8.43×10^{-11}	6.44×10^{-10}	175.96	277.96
110	1483	6.46×10^{-11}	1.66×10^{-11}	4.80×10^{-11}	6.29×10^{-10}	176.16	278.26
						ave.	279.5 ± 3.1

Table 6
Analysis of thermodynamic data for the reaction $PuO_2 \cdot xSiO_2(s) + 1/2O_2(g) + H_2O(g) = xSiO_2(gl) + PuO_2(OH)_2(g)$

Run #	T (K)	p(Pu total) (bar	$p(PuO_3)$ (bar)	$p(PuO_2(OH)_2)$ (bar)	K_{eq} (J/mol K)	$\Delta_r G_r^0/T$ (kJ/mol)	$\Delta_r H_{298}^0$
$^{238}PuO_2$(s), with filter:							
77	1327	5.59×10^{-14}	1.14×10^{-14}	4.32×10^{-14}	1.16×10^{-13}	247.63	345.32 [a]
85	1326	3.18×10^{-14}	1.23×10^{-14}	1.96×10^{-14}	5.26×10^{-14}	254.23	353.85 [a]
91	1326	7.79×10^{-13}	4.51×10^{-15}	7.75×10^{-13}	4.26×10^{-12}	217.68	305.39
92	1326	2.80×10^{-13}	6.76×10^{-15}	2.73×10^{-13}	2.04×10^{-12}	223.82	313.52
93	1325	5.47×10^{-15}	7.30×10^{-15}				
94	1326	4.25×10^{-14}	7.99×10^{-15}	3.45×10^{-14}	8.56×10^{-13}	231.03	323.08
95	1325	1.34×10^{-14}	4.40×10^{-15}	8.97×10^{-15}	4.92×10^{-14}	254.78	354.31 [a]
96	1325	3.14×10^{-14}	7.70×10^{-15}	2.37×10^{-14}	5.62×10^{-13}	234.53	327.47
112	1486	4.82×10^{-11}	1.74×10^{-12}	4.65×10^{-11}	1.28×10^{-10}	189.33	298.40
115	1486	1.03×10^{-12}	1.24×10^{-12}				
$^{239}PuO_2$(s), with filter:							
101	1431	1.12×10^{-12}	1.33×10^{-13}	9.93×10^{-13}	5.44×10^{-12}	215.65	325.56
102	1431	7.14×10^{-12}	1.94×10^{-13}	6.95×10^{-12}	5.09×10^{-11}	197.07	298.97
103	1431	2.41×10^{-12}	2.20×10^{-13}	2.19×10^{-12}	2.93×10^{-11}	201.65	305.52
						ave.	312.2 ± 11.9

[a] These values are not included in determining the average $\Delta H_{r,298}^0$.

Data for Eq. (5) for $PuO_2(OH)_2(g)$ volatility from $PuO_2 \cdot xSiO_2(s)$ are summarized in Table 6. This is the case where both oxygen and steam are present and the silica wool filter is used. Values of $p(PuO_3)$ are calculated for each data point using the thermodynamic data from Eq. (4), and $p(PuO_3)$ is subtracted from p(Pu total) to obtain $p(PuO_2(OH)_2)$ values. Several data points cannot be used because $p(PuO_2(OH)_2)$ comes out negative, or the values appear to be spuriously low. The data are illustrated in Fig. 4 as a $\log K_{eq}$ versus $1/T$ plot. The $p(PuO_2(OH)_2)$ values show a large scatter, but are down by about a factor of 20 as compared with Eq. (1). $\Delta_r H^0_{298}$ is found to be (312.2 ± 11.9) kJ/mol.

The thermodynamics for the reaction

$$PuO_2(s) + xSiO_2(gl) = PuO_2(s) \cdot xSiO_2(s) \qquad (6)$$

may be obtained by subtracting Eq. (4) from Eq. (2) and also by subtracting Eq. (5) from Eq. (1). Thus, from Eqs. (2) and (4), $\Delta_r H^0_{298} = (493.0 \pm 4.8) - (528.2 \pm 22.5) = -(35.1 \pm 23.0)$ kJ/mol, and from Eqs. (1) and (5), $\Delta H^0_{r,298} = (279.5 \pm 3.1) - (312.2 \pm 11.9) = -(32.8 \pm 12.3)$ kJ/mol. The agreement is fortuitously good considering the large amount of scatter in the data. As a best value $\Delta_r H^0_{298} = -(33.5 \pm 17.0)$ kJ/mol. For large x, the $(\Delta_r G^0_T - \Delta_r H^0_{298})/T$ values approach zero for this reaction, so that $\Delta_r G^0_T = \Delta_r H^0_{298}$. In other words, $\Delta_r S^0_T$ for Eq. (6) is expected to be approximately zero. The nature of the Pu and silica wool interaction is not clear. However, SiO_2(gl) is in large excess and the interaction may only be due to a surface compound. The amount of volatile Pu species passed through is the wool much less than required to form a monolayer, i.e., about 200 μg of PuO_2 would be required to form a monolayer on the silica wool surface in our experiment. The compound may also be a result of impurities volatilizing out of the furnace that interact with PuO_2(s). Therefore, it is not suggested that the extent of reaction found here between silica wool and the gaseous Pu species represents the degree of reaction between PuO_2(s) and SiO_2(gl) when PuO_2(s) is present in greater concentrations.

It was also possible to measure U volatilities in the $^{238}PuO_2$(s) runs, since ^{234}U was present as a decay product at 3.3 at.% of the ^{238}Pu in the $^{238}PuO_2$(s). Analyses were therefore carried out for ^{234}U in the collection samples. Results for volatility of ^{234}U in the $^{238}PuO_2$(s) runs are

Table 7
Volatility of ^{234}U observed in transpiration experiments on $^{238}PuO_2$(s). Experimental conditions are the same as those given for the runs in Table 1. The observed ^{234}U volatilities are compared with volatilities calculated from U_3O_8(s)

Run #	T (K)	^{234}U (μg)	Measured pU(tot) (bar)	Calculated pU(tot) (bar)	pU(tot) meas./pU(tot) calc.
77	1327	14.5	2.37×10^{-8}	1.34×10^{-7}	0.177
78	1325	5.96	2.09×10^{-8}	9.64×10^{-8}	0.217
79	1327	8.99	2.25×10^{-8}	9.03×10^{-8}	0.249 [b]
80	1326	12.3	2.45×10^{-8}	7.84×10^{-8}	0.313 [b]
85	1326	7.97	1.62×10^{-8}	1.30×10^{-7}	0.125
86	1326	1.82	6.36×10^{-9}	9.88×10^{-8}	0.064
87	1326	5.43	1.28×10^{-8}	8.81×10^{-8}	0.145
88	1326	4.57	1.11×10^{-8}	7.51×10^{-8}	0.148
91	1326	4.65	5.12×10^{-9}	1.03×10^{-7}	0.050
92	1326	2.61	6.45×10^{-9}	9.42×10^{-8}	0.068
93	1325	2.12	6.55×10^{-9}	8.47×10^{-8}	0.077
94	1326	0.833	5.69×10^{-9}	8.16×10^{-8}	0.070
95	1325	3.99	4.48×10^{-9}	1.01×10^{-7}	0.044
96	1325	1.04	3.78×10^{-9}	7.98×10^{-8}	0.047
105 [a]	1482	19.1	1.30×10^{-7}	3.22×10^{-6}	0.040
106 [a]	1482	20.5	3.58×10^{-7}	3.28×10^{-6}	0.109
107 [a]	1483	18.3	6.39×10^{-7}	3.34×10^{-6}	0.191
108 [a]	1482	27.8	1.59×10^{-7}	2.39×10^{-6}	0.066
109 [a]	1483	17.0	2.14×10^{-7}	2.59×10^{-6}	0.082
110 [a]	1483	17.0	2.65×10^{-7}	2.60×10^{-6}	0.102
111 [a]	1483	16.9	3.94×10^{-7}	3.34×10^{-6}	0.118
112	1486	21.7	1.88×10^{-7}	3.50×10^{-6}	0.054
113	1487	21.0	3.67×10^{-7}	3.62×10^{-6}	0.101
114	1485	14.1	4.92×10^{-7}	3.49×10^{-6}	0.142
115	1486	31.6	2.76×10^{-7}	3.26×10^{-6}	0.085
116	1485	0.0045	8.56×10^{-11}	0	
				ave.	0.10 ± 0.05

[a] These runs were made without a silica glass wool dust filter.
[b] These values are not included in determining the average(pU(tot) meas.)/(pU(tot) calc.).

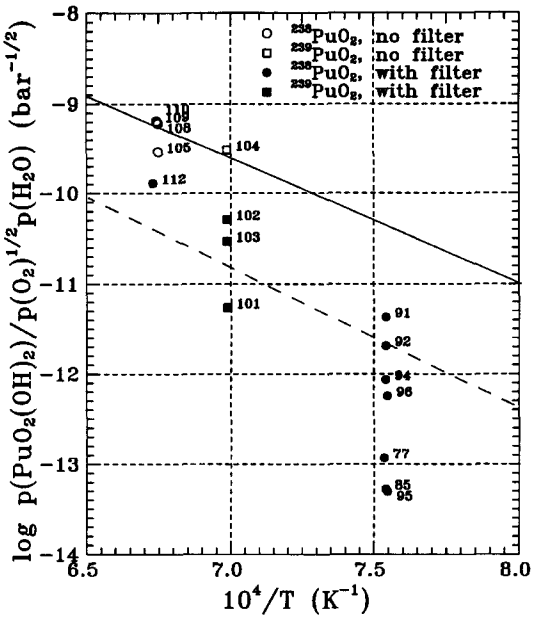

Fig. 4. Plots of log $p(PuO_2(OH)_2)/p(O_2)^{1/2}p(H_2O)$ versus $1/T$ for the reactions: $PuO_2(s)+1/2O_2(g)+H_2O(g)=PuO_2(OH)_2(g)$ (with no silica glass wool filter) and $PuO_2\cdot xSiO_2(s)+1/2O_2(g)+H_2O(g)=xSiO_2(gl)+PuO_2(OH)_2(g)$ (with silica glass wool filter).

summarized in Table 7. Comparing these U volatilities with Pu volatilities in Table 1 shows that U volatilities are about 10^4 times higher than the Pu volatilities. In contrast to the Pu volatility data, no significant difference in the data is seen with or without the silica glass wool filter, thus indicating no significant interaction of U with silica or that at higher vapor pressures the interaction is insignificant. The observed U volatilities are compared with the sum of the expected pressures of $UO_3(g)$ and $UO_2(OH)_2(g)$ over $U_3O_8(s)$ from the thermodynamic data of Ref. [4] (see Table 7). Measured uranium pressures are lower than calculated and show a fair amount of scatter. The average ratio of measured to calculated U pressures is (0.10 ± 0.05). The measured uranium pressures are expected to be less than calculated if $U_3O_8(s)$ is not present as a pure solid, but in solid solution in $PuO_2(s)$, and hence at a reduced activity. Phase diagram information shows for $U_3O_8(s)$–$PuO_2(s)$ samples heated in air at 1023 to 1123K, the solubility limit of $UO_{2.67}(s)$ (i.e., $1/3$ $U_3O_8(s)$) in $PuO_2(s)$ is about 14 mol%, and the solubility limit of $PuO_2(s)$ in $UO_{2.67}(s)$ is about 9 mol% [8]. Because of the existence of limited mutual solubilities of $U_3O_8(s)$ and $PuO_2(s)$, the solution of $UO_{2.67}(s)$ in $PuO_2(s)$ is not ideal. The activity of $UO_{2.67}(s)$ in the $PuO_2(s)$ phase is expected to increase more rapidly with concentration than in an ideal solution because the $UO_{2.67}(s)$ activity should be close to unity at 14 mol% $UO_{2.67}(s)$, i.e., at the two-phase boundary. For the sample of $^{238}PuO_2(s)$ which contains 3.3 mol% $^{234}UO_{2.67}$, the ideal $UO_{2.67}(s)$ activity would be 0.033. Based upon the observed ratio of (pU(tot) meas.)/(pU(tot) calc.) of (0.10 ± 0.05), the $UO_{2.67}(s)$ activity is therefore (0.10 ± 0.05), which at three times the ideal solution activity is a reasonable value.

4. Application to thermal oxidation processors

As an example of the $PuO_3(g)$ and $PuO_2(OH)_2(g)$ volatility contributions to air emissions, modelling is now carried out for incineration of Pu-contaminated laboratory mixed waste solids. The volatilities are only calculated for Pu species resulting from the presence of oxygen and steam. Unknown Pu volatilities induced by chlorine and fluorine are not included. The calculations are made for a variety of combustion temperatures. The amount of carry-over of Pu in flyash is also estimated by making a number of assumptions about Pu content in the feed, mass flow rates, and flyash recovery by air pollution control equipment. A particular incinerator operation can differ in these details, but the illustration should be useful in giving an estimate of the behavior. The thermodynamic data can similarly be applied to model emissions in other types of thermal oxidation processors depending upon the specific operational conditions.

The incinerator is taken to have a primary and secondary combustor, i.e., afterburner. The secondary combustor is operated at a higher temperature (greater than 1000°C whereas the primary combustor would normally be operated at less than 1000°C), and the presence of $PuO_2(s)$ in flyash in the secondary combustor is assumed to set the level of Pu volatility. The input waste feed rate is taken to be 100 kg/h, with a Pu content of 100 ppm in the waste. This waste feed rate is in a range that would be appropriate for pilot scale process in industry, but would be more than adequate to treat transuranic wastes generated from a DOE facility. A Pu content of 100 ppm is in a range that would be expected for standard glove box waste. 50 kg/h of bottom ash and 3 kg/h of flyash are assumed to be produced in the two-stage combustion. These numbers are typical of rotary kiln incinerators where a limited amount of volatiles are generated and recondense in the offgas. The offgas flow out of the secondary combustor is taken to be 220 kg/h. If 47 kg/h or combustible wastes in the primary combustor and a significant amount of excess air is used and if in the secondary combustor more fuel and air are added, the total offgas flow rate becomes about 220 kg/h. The $O_2(g)$ and $H_2O(g)$ pressures in the secondary combustor offgas are taken at 0.1 bar each, and the average molecular weight of the offgas is assumed to be 35. Water and oxygen compositions are consistent with an operation using about 100% excess air in the primary and secondary combustors and the molecular weight is consistent with a offgas composition composed of a large frac-

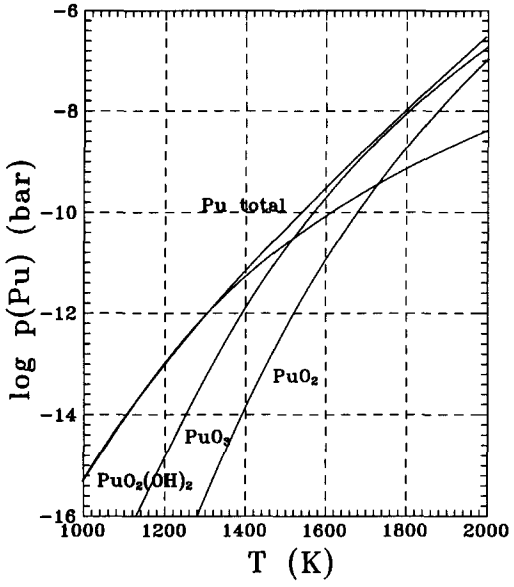

Fig. 5. Calculated pressures of Pu species above PuO_2(s) in the presence of 0.1 bar each of O_2(g) and H_2O(g) as a function of temperature.

tion of N_2(g) and CO_2(g) with lesser amounts of O_2(g) and H_2O(g). Several air pollution control devices are used in sequence to remove the flyash, with HEPA filters being used for the final removal of fine particulates. Being non-specific about the front end air pollution control devices used (e.g., cyclones, fabric filters, venturi scrubbers, ionizing scrubbers, electrostatic precipitators, etc.), it is assumed that particulates greater than 5 μm and comprising 99% (assumes no volatiles like PbO in the waste stream) of the flyash mass are removed by the front end air pollution control devices, and then the offgas is passed through HEPA filters where 99.98% of the remaining fines are removed before release of the offgas to the air.

Pressures of PuO_3(g) and $PuO_2(OH)_2$(g) are calculated according to Eqs. (1) and (2) and using the thermodynamic data given in this report (see Table 8 and Fig. 5). Pressures of PuO_2(g) are also included in Table 8 and Fig. 5, according to the reaction and equilibrium constant

$$PuO_2(s) = PuO_2(g), \quad K_7 = p(PuO_2)/a(PuO_2), \tag{7}$$

and using thermodynamic data given by Cordfunke et al. [6]. The Pu volatility results principally from $PuO_2(OH)_2$(g) at temperatures below 1350 K, a mixture of $PuO_2(OH)_2$(g) and PuO_3(g) at 1350–1700 K, and a mixture of PuO_3(g) and PuO_2(g) above 1700 K. Total Pu species pressures are also given in Table 8 and Fig. 5.

The mass rate of volatilized Pu exiting in the combustion chamber is determined as follows. From the ideal gas law,

$$pV = nRT = (w/M)RT, \tag{8}$$

and for conditions of constant volume and temperature,

$$w_{Pu}/w_{og} = M_{Pu}\, p_{Pu}/M_{og}\, p_{og}, \tag{9}$$

where og refers to the offgas. In terms of g Pu/h for the incinerator described here,

$$\begin{aligned} g\ \text{Pu/h} &= (g\ \text{og/h})M_{Pu}\, p(\text{Pu total})/M_{og}\, p_{og} \\ &= (2.20\times 10^5)(239)\, p(\text{Pu total})/(35)(1.01) \\ &= 1.48\times 10^6 p(\text{Pu total}). \end{aligned} \tag{10}$$

Upon cooldown of the offgas, the volatilized Pu is expected to condense out primarily on fine ash particulates, i.e., on particulates less than 1 μm in size. Thus, the amounts of Pu resulting from volatilized Pu are calculated by Eq. (10) as the amounts of Pu carryover in fine particulates in the cooled offgas prior to passing through the HEPA filter (see Table 8 and Fig. 5). This volatility contribution of Pu in fine particulates can be compared with the amount of Pu carried over as non-volatilized

Table 8
Pu volatility as a function of incinerator combustion temperature. Sufficient Pu is assumed to be available in the feed to form PuO_2(s) in the combustion ash, O_2(g) and H_2O(g) pressures are taken to be 0.1 bar each, and the combustion offgas flowrate is 220 kg/h. Calculated values are given for pressures of each of the gaseous Pu species and for the total Pu pressure. Also given is the calculated amount of Pu condensate carried in fine particulates (< 1 μm) in the cooled offgas

T (K)	$p(PuO_2(OH)_2)$ (bar)	$p(PuO_3)$ (bar)	$p(PuO_2)$ (bar)	$p(Pu_{total})$ (bar)	g Pu/h carry-over in fines
1000	5.0×10^{-16}	1.1×10^{-19}	6.6×10^{-24}	5.0×10^{-16}	7.38×10^{-10}
1100	9.6×10^{-15}	2.0×10^{-17}	6.5×10^{-21}	9.7×10^{-15}	1.43×10^{-8}
1200	1.1×10^{-13}	1.5×10^{-15}	2.0×10^{-18}	1.1×10^{-13}	1.70×10^{-7}
1300	8.9×10^{-13}	5.8×10^{-14}	2.4×10^{-16}	9.5×10^{-13}	1.40×10^{-6}
1400	5.1×10^{-12}	1.3×10^{-12}	1.5×10^{-14}	6.5×10^{-12}	9.60×10^{-6}
1500	2.3×10^{-11}	1.9×10^{-11}	5.2×10^{-13}	4.3×10^{-11}	6.37×10^{-5}
1600	8.7×10^{-11}	2.0×10^{-10}	1.1×10^{-11}	2.9×10^{-10}	4.37×10^{-4}
1700	2.7×10^{-10}	1.5×10^{-9}	1.7×10^{-10}	2.0×10^{-9}	2.90×10^{-3}
1800	7.6×10^{-10}	9.2×10^{-9}	1.9×10^{-9}	1.2×10^{-8}	1.76×10^{-2}
1900	1.9×10^{-9}	4.6×10^{-8}	1.6×10^{-8}	6.4×10^{-8}	9.43×10^{-2}
2000	4.1×10^{-9}	1.9×10^{-7}	1.1×10^{-7}	3.0×10^{-7}	4.52×10^{-1}

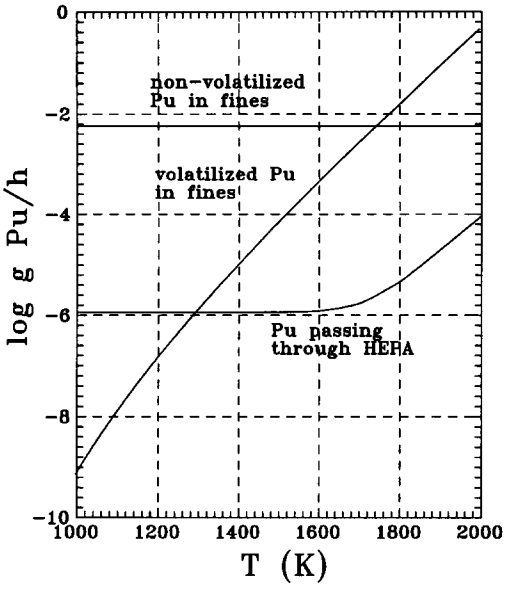

Fig. 6. Calculated amounts of volatilized Pu carryover in particulates of < 1 μm size and non-volatilized $PuO_2(s)$ in particulates of < 5 μm size in the incinerator offgas as a function of combustor temperature. Amounts of Pu passing through HEPA filters are also shown.

$PuO_2(s)$ in the fine flyash particulates prior to the HEPA filter. The proportion of ash in these fine particulates to total ash is $(0.01 \times 3 \text{ kg/h})/(53 \text{ kg/h}) = 5.7 \times 10^{-4}$, which, multiplied by 0.01 kg Pu/h in the input waste, gives 5.7 mg Pu/h as non-volatilized $PuO_2(s)$ carryover in fine ash particulates. This contribution (shown in Fig. 6) is independent of combustion temperature. It can be seen in Fig. 6 that the volatilized- and non-volatilized-Pu contributions become equal at a combustion temperature of 1735 K. If the secondary combustion temperature is maintained below 1600 K (secondary combustion temperature is normally less than 1500 K), volatilization of Pu should not significantly enhance Pu emissions beyond that carried as $PuO_2(s)$ in the fine flyash particulates. Importantly, HEPA filters will remove 99.98% of the fines. Pu emission rates after passing through HEPA filters are also shown in Fig. 6. Thus, by maintaining the secondary combustion temperature below 1600 K, Pu emission rates are estimated to be 1.1 μg Pu/h, an amount set by physical entrainment factors and not by volatilization and condensation processes. Although emission rates are calculated for a relatively specific set of conditions, they would have to change dramatically for plutonium volatility to become significant at the temperatures incinerators normally operate.

Acknowledgements

The authors would like to acknowledge the valuable assistance of Ronald W. Lougheed and Kenton J. Moody for performing radiochemical analyses on the collected samples and George Rizeq of Energy Environment Research Corporation for helpful comments and discussion on the application of the volatility data to thermal oxidation processors.

References

[1] R.G. Rizeq, D.W. Hansell, W. Clark, L. Pooler, W.R. Seeker, The Behavior of Metals in Hazardous Waste Combustion Systems, FY92 Final Report, Hazardous Waste Combustion Systems Metals Bible, Energy and Environmental Research Corporation, 18 Mason, Irvine, CA, 1992.

[2] R.G. Rizeq, D.W. Hansell, W. Clark, W.R. Seeker, Predictions of Metals Emissions from Hazardous Waste Incinerators and Comparison to Test Results from a Full Scale Facility, in C. Baker, E. McDaniel, J. Tripodes (Eds.), Proc. of the 1993 Incineration Conf. at Knoxville, Tennessee, May 3–7, 1993, Univ. of California, EH&S, Irvine, CA, 1993, pp. 817–822.

[3] O.H. Krikorian, R.H. Condit, A.F. Fontes, Jr., D.L. Fleming, J.W. Magana, W.F. Morris, M.G. Adamson, Measurement of Plutonium and Americium Volatilities under Thermal Process Conditions: Final Report, Lawrence Livermore National Laboratory Report, UCRL-ID-112994, 1993.

[4] O.H. Krikorian, B.B. Ebbinghaus, Martyn G. Adamson, Alfred S. Fontes Jr., D.L. Fleming, Experimental Studies and Thermodynamic Modeling of Volatilities of Uranium, Plutonium, and Americium from Their Oxides and from Their Oxides Interacted with Ash, Lawrence Livermore National Laboratory Report, UCRL-ID-114774, 1993.

[5] F.D. Richardson, C.B. Alcock, in: Physicochemical Measurements at High Temperatures, ed. J. O'M. Bockris, J.L. White and J.D. Mackenzie (Butterworths, London, 1959) p. 135.

[6] E.H.P. Cordfunke, R.J.M. Konings, P.E. Potter, G. Prins, M.H. Rand, in: Thermochemical Data for Reactor Materials and Fission Products, ed. E.H.P. Cordfunke and R.J.M. Konings (North-Holland, Amsterdam, 1990).

[7] B.B. Ebbinghaus, Calculated Thermodynamic Functions for Gas Phase Uranium, Neptunium, Plutonium, and Americium Oxides (AnO_3), Oxyhydroxides ($AnO_2(OH)_2$), Oxychlorides (AnO_2Cl_2), and Oxyfluorides (AnO_2F_2), report to be issued.

[8] T.L. Markin, R.S. Street, J. Inorg. Nucl. Chem. 29 (1967) 2265.

[9] S.R. Dharwadkar, S.N. Tripathi, M.D. Karkhanavala, M.S. Chandrasekharaiah, Proc. Thermodynamics of Nuclear Materials, Vol. II, Agency, Vienna, Austria, 1974, pp. 455–465.